Measurement of polarization observables for Λ hyperon.

Shankar Adhikari

Florida International University

15 November 2018

Outline

Outline

1. Introduction
   - Missing Baryon Problem
2. Experiment and Data Analysis
   - Experiment
   - Data Analysis
   - Measurement method
3. Results and Summary
   - Results comparison
   - Systematic uncertainty
   - Summary

Missing Baryon Problem

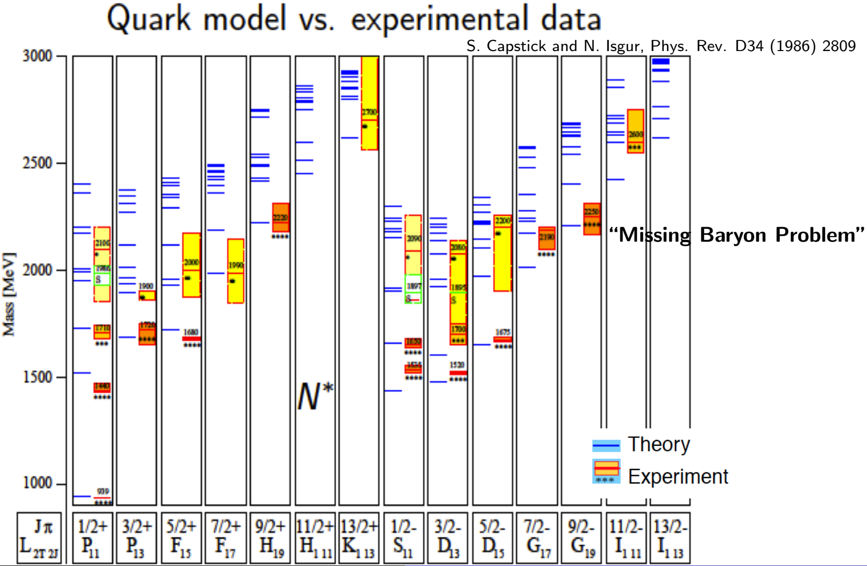

Missing Baryon Problem and $K^+\Lambda$ channel

From an experimental point-of-view;

- Pion beams was the primary tool to study resonances. It is predicted that the high-mass resonances predominantly couple to γ beams.

Missing Baryon Problem and $K^+\Lambda$ channel

From an experimental point-of-view;

- Pion beams was the primary tool to study resonances. It is predicted that the high-mass resonances predominantly couple to γ beams.
- Not all resonances couple strongly to the $N\pi$ channel; coupled to other channels as well.
- Interference of states: Resonances are broad and overlapping, possible interference between N and Δ states.

Particle	J^P	overall	Status as seen in									
			$N\gamma$	$N\pi$	$\Delta\pi$	$N\sigma$	$N\eta$	ΛK	ΣK	$N\rho$	$N\omega$	$N\eta\prime$
N	$1/2^+$	****										
$N(1440)$	$1/2^+$	****	****	****	****	***						
$N(1520)$	$3/2^-$	****	****	****	****	**	****					
$N(1535)$	$1/2^-$	****	****	****	***	*	****					
$N(1650)$	$1/2^-$	****	****	****	***	*	****	*				
$N(1675)$	$5/2^-$	****	****	****	****	***	*	*	*			
$N(1680)$	$5/2^+$	****	****	****	****	***	*	*	*			
$N(1700)$	$3/2^-$	***	**	***	***	*	*			*		
$N(1710)$	$1/2^+$	****	****	****	*		***	**	*	*	*	
$N(1720)$	$3/2^+$	****	****	****	***	*	*	****	*	*	*	
$N(1860)$	$5/2^+$	**	*	**		*	*					
$N(1875)$	$3/2^-$	***	**	**	*	**	*	*	*	*	*	
$N(1880)$	$1/2^+$	***	**	*	**	*	*	**	**		**	
$N(1895)$	$1/2^-$	****	****	*	*	*	****	**	**	*	*	****
$N(1900)$	$3/2^+$	****	****	**	**	*	*	**	**		*	**
$N(1990)$	$7/2^+$	**	**	**			*	*	*			
$N(2000)$	$5/2^+$	**	**	*	**	*	*				*	
$N(2040)$	$3/2^+$	*		*								
$N(2060)$	$5/2^-$	***	***	**	*	*	*	*	*	*	*	
$N(2100)$	$1/2^+$	***	**	***	**	**	*	*		*	*	**
$N(2120)$	$3/2^-$	***	***	**	**	**						
$N(2190)$	$7/2^-$	****	****	****	****	**						
$N(2220)$	$9/2^+$	****	**	****								
$N(2250)$	$9/2^-$	****	**	****								
$N(2300)$	$1/2^+$	**		**								
$N(2570)$	$5/2^-$	**		**								
$N(2600)$	$11/2^-$	***		***								
$N(2700)$	$13/2^+$	**		**								

**** Existence is certain.
*** Existence is very likely.
** Evidence of existence is fair.
* Evidence of existence is poor.

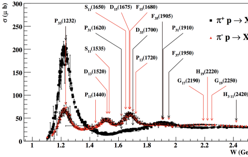

Particle Data Group 2018.

Missing Baryon Problem and $K^+\Lambda$ channel

From an experimental point-of-view;

- Pion beams was the primary tool to study resonances. It is predicted that the high-mass resonances predominantly couple to γ beams.
- Not all resonances couple strongly to the $N\pi$ channel; coupled to other channels as well.
- Interference of states: Resonances are broad and overlapping, possible interference between N and Δ states.
- $\gamma p \to K^+\Lambda$ channel is important that;

  - only contribute to N^* with $I = 1/2$.

  - $\Lambda \to p\pi^-$, self-analyzing nature of Λ hyperon allow us to measure polarization observables from its decay products

			Status as seen in									
Particle	J^P	overall	$N\gamma$	$N\pi$	$\Delta\pi$	$N\sigma$	$N\eta$	ΛK	ΣK	$N\rho$	$N\omega$	$N\eta'$
N	$1/2^+$	****										
$N(1440)$	$1/2^+$	****	****	****	****	***						
$N(1520)$	$3/2^-$	****	****	****	****	**	****					
$N(1535)$	$1/2^-$	****	****	****	***	*	****					
$N(1650)$	$1/2^-$	****	****	****	***	*	****	*				
$N(1675)$	$5/2^-$	****	****	****	****	***	*	*	*			
$N(1680)$	$5/2^+$	****	****	****	****	***	*	*	*			
$N(1700)$	$3/2^-$	***	**	***	***	*	*			*		
$N(1710)$	$1/2^+$	****	****	****	*		***	**	*	*	*	
$N(1720)$	$3/2^+$	****	****	****	***	*	*	****	*	*	*	
$N(1860)$	$5/2^+$	**	*	**		*	*					
$N(1875)$	$3/2^-$	***	**	**	*	**	*	*	*	*	*	
$N(1880)$	$1/2^+$	***	**	*	**	*	*	**	**		**	
$N(1895)$	$1/2^-$	****	****	*	*	*	****	**	**	*	*	****
$N(1900)$	$3/2^+$	****	****	**	**	*	*	**	**		*	**
$N(1990)$	$7/2^+$	**	**	**			*	*	*			
$N(2000)$	$5/2^+$	**	**	*	**	*	*				*	
$N(2040)$	$3/2^+$	*		*								
$N(2060)$	$5/2^-$	***	***	**	*	*	*	*	*	*	*	
$N(2100)$	$1/2^+$	***	**	***	**	**	*	*		*	*	**
$N(2120)$	$3/2^-$	***	***	**	**	**		**	*		*	*
$N(2190)$	$7/2^-$	****	****	****	****	**	*	**	*	*	*	
$N(2220)$	$9/2^+$	****	**	****			*	*	*			
$N(2250)$	$9/2^-$	****	**	****			*	*	*			
$N(2300)$	$1/2^+$	**		**								
$N(2570)$	$5/2^-$	**		**								
$N(2600)$	$11/2^-$	***		***								
$N(2700)$	$13/2^+$	**		**								

**** Existence is certain.
*** Existence is very likely.
** Evidence of existence is fair.
* Evidence of existence is poor.

... polarization observables are sensitive to the interefence from different states and different processes

Polarization observables

Photoproduction of pseudoscalar meson; 16 total measurement, at least 8 measurement requires.

$$
\begin{aligned}
d\sigma = \frac{1}{2}\Big(& d\sigma_0 + \hat{\Sigma}[-P_L^\gamma \cos(2\phi_\gamma)] + \hat{T}[P_y^T] + \hat{P}[P_{y'}^R] \\
&+\hat{E}[-P_c^\gamma P_z^T] + \hat{G}[P_L^\gamma P_z^T \sin(2\phi_\gamma)] + \hat{F}[P_c^\gamma P_x^T] + \hat{H}[P_L^\gamma P_x^T \sin(2\phi_\gamma)] \\
&+\hat{C}_{x'}[P_c^\gamma P_{x'}^R] + \hat{C}_{z'}[P_c^\gamma P_{z'}^R] + \hat{O}_{x'}[P_L^\gamma P_{x'}^R \sin(2\phi_\gamma)] + \hat{O}_{z'}[P_L^\gamma P_{z'}^R \sin(2\phi_\gamma)] \\
&+ \hat{L}_{x'}[P_z^T P_{x'}^R] + \hat{L}_{z'}[P_z^T P_{z'}^R] + \hat{T}_{x'}[P_x^T P_{x'}^R] + \hat{T}_{z'}[P_x^T P_{z'}^R]\Big).
\end{aligned}
$$

Polarized	Beam			Target			Hyperon		
	unpol.	linear	circular	x	y′	z	x′	y′	z′
Unpolar.	σ								
Beam:		Σ							
linear				H		G	$O_{x'}$		$O_{z'}$
circular				F		E	$C_{x'}$		$C_{z'}$
Target:					T				
x							$T_{x'}$		$T_{z'}$
z							$L_{x'}$		$L_{z'}$
Hyperon:								P	

Polarization observables

With C_x, C_z, and P

$$\frac{d\sigma}{d\Omega} \equiv \sigma(\cos\theta_x, \cos\theta_y, \cos\theta_z)$$

$$= \sigma_\circ\{1 + \alpha P^\gamma C_x \cos\theta_x$$

$$+ \alpha P^\gamma C_z \cos\theta_z + \alpha P \cos\theta_y\}$$

Polarized	Beam			Target			Hyperon		
	unpol.	linear	circular	x	y′	z	x′	y′	z′
Unpolar.	σ								
Beam:		Σ							
linear				H		G	$O_{x'}$		$O_{z'}$
circular				F		E	$C_{x'}$		$C_{z'}$
Target:					T				
x							$T_{x'}$		$T_{z'}$
z							$L_{x'}$		$L_{z'}$
Hyperon:								P	

Polarization observables

With C_x, C_z, and P

$$\frac{d\sigma}{d\Omega} \equiv \sigma(\cos\theta_x, \cos\theta_y, \cos\theta_z)$$
$$= \sigma_\circ\{1 + \alpha P^\gamma C_x \cos\theta_x$$
$$+\alpha P^\gamma C_z \cos\theta_z + \alpha P \cos\theta_y\}$$

Polarized	Beam	Target	Hyperon
	unpol. linear circular	x y′ z	x′ y′ z′
Unpolar.	σ		
Beam: linear circular	Σ	 H G F E	 $O_{x'}$ $O_{z'}$ $C_{x'}$ $C_{z'}$
Target: x z		T	 $T_{x'}$ $T_{z'}$ $L_{x'}$ $L_{z'}$
Hyperon:			P

How to measure? $\gamma p \to K^+\Lambda$

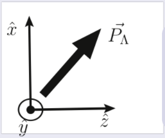

$$P_{\Lambda_z} = P_\odot C_z, \text{ along } \hat{z}$$
$$P_{\Lambda_y} = P, \text{ along } \hat{y}$$
$$P_{\Lambda_x} = P_\odot C_x, \text{ along } \hat{x}$$

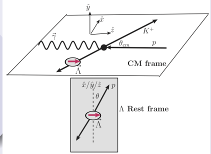

$$\hat{z} = \hat{p}_\gamma$$
$$\hat{y} = \frac{\hat{p}_\gamma \times \hat{p}_K}{|\hat{p}_\gamma \times \hat{p}_K|}$$
$$\hat{x} = \hat{y} \times \hat{z}$$

Establishing the N^* - $N(1900)3/2^+$

- Bump first seen in SAPHIR $K^+\Lambda$ cross section data but due to systematic, misinterpreted as $J^p = 3/2^-$ for $J^p = 3/2^+$
- Established in BnGa multichannel analysis using CLAS cross section and polarization results (C_x and C_z), $J^p = 3/2^+$ let to the $***$ in PDG2012, PDG2018 $****$.

  R. Bradford et al. [CLAS Collaboration], PRC 75, 035205 (2007)
- First baryon resonance observed and confirmed in electromagnetic meson production.

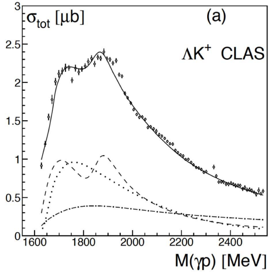

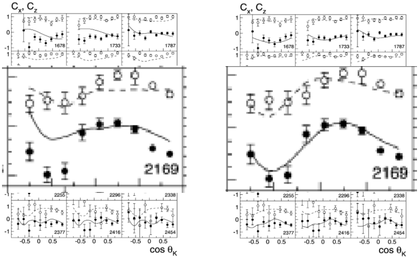

What is significance?

- $\gamma p \rightarrow K^+\Lambda$; resonant and non-resonant process. Significant background from non-resonant processes which are entangled with resonant processes. Crucial to understand non-resonant process.
- C_x and C_z: E_γ up to 5.45 Gev or W up to 3.33 GeV (previously 2.5 GeV)
- P: W up to 3.33 GeV (previously 2.8 GeV)

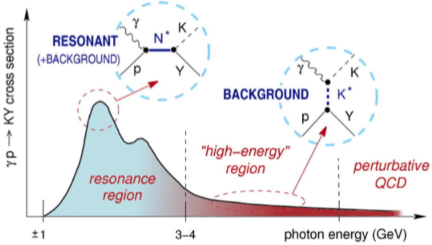

credit: T. Corthals

Outline

g12 Experiment using CLAS @ JLab

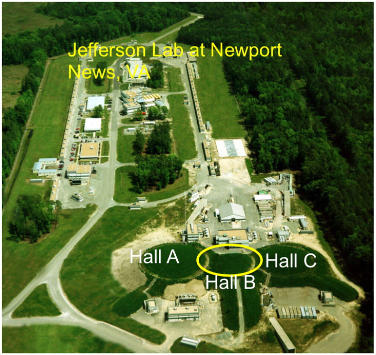

Hall B spectrometer

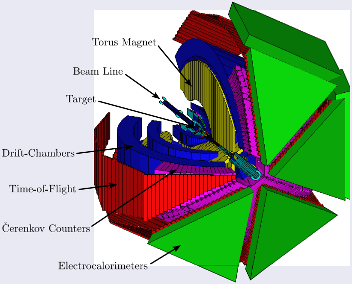

g12 experiment

Photon Pol: Circular
Target Material ℓH_2
Target Position -90 cm from CLAS center

E_γ **range**: 1.142 – 5.45 GeV

$\gamma p \to K^+\Lambda \to K^+ p\pi^-$

- Topologies for $K^+ p\pi^-$
  three-track: $\gamma p \to K^+ p\pi^-$ (no missing particle)
  two-track: $\gamma p \to K^+ p$ (missing π^-)
- Standard cuts and corrections
  g12 analysis note
  - Timing cut
  - Vertex cut
  - Fiducial cut
  - Time of Flight Knockout
  - Multiple Photon Cut
  - E-p corrections

$\gamma p \to K^+\Lambda$, Λ decay mode

$p\pi^- \to 64\%$ $n\pi^\circ \to 36\%$.

Final state K^+, proton, and π^- are required in data.

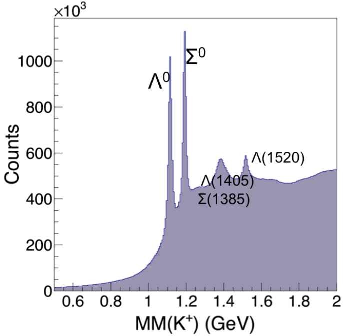

$\gamma p \to K^+\Lambda \to K^+ p\pi^-$

- Topologies for $K^+p\pi^-$
  three-track: $\gamma p \to K^+p\pi^-$ (no missing particle)
  two-track: $\gamma p \to K^+p$ (missing π^-)
- Standard cuts and corrections
  g12 analysis note
  - Timing cut
  - Vertex cut
  - Fiducial cut
  - Time of Flight Knockout
  - Multiple Photon Cut
  - E-p corrections
- After cuts and corrections

Example: vertex cut

Cut within the target length, z-vertex 40 cm + 5 cm downstream, radial r <5 cm.

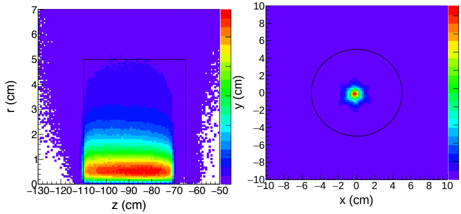

$\gamma p \to K^+\Lambda \to K^+ p\pi^-$

- Topologies for $K^+ p\pi^-$
  three-track: $\gamma p \to K^+ p\pi^-$ (no missing particle)
  two-track: $\gamma p \to K^+ p$ (missing π^-)
- Standard cuts and corrections
  g12 analysis note
  – Timing cut
  – Vertex cut
  – Fiducial cut
  – Time of Flight Knockout
  – Multiple Photon Cut
  – E-p corrections
- After cuts and corrections

two-track

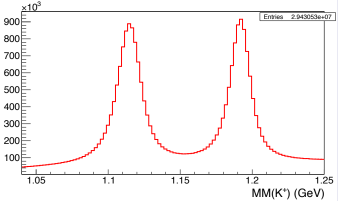

three-track

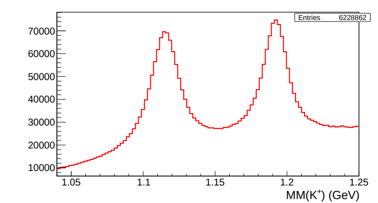

Kinematic Fitting

two-track

$\gamma p \rightarrow K^+ p(\pi^-)$; hypothesis
$CL > 5\%$

three-track

$\gamma p \rightarrow K^+ p\pi^-$; hypothesis
$CL > 1\%$

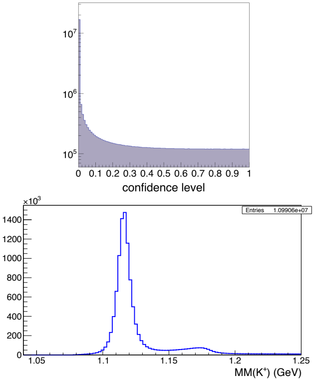

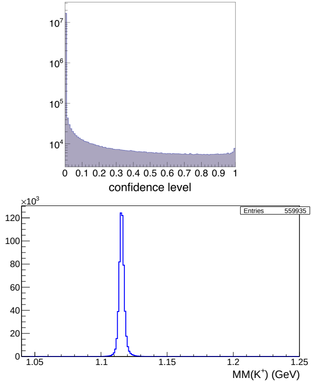

Event based dilution factor calculation for $\gamma p \rightarrow K^+ p(missing \pi^-)$

- Energy dependent MM(K^+)
- Q-factor method (A multivariant analysis)

  For each event ("seed event"), find N nearest neighbors in kinematic phase space (e.g. $\cos\theta_{K^+}^{cm}$, $\cos\theta_p^{cm}$, ϕ_p and W). Plot mass distribution of the $N+1$ events and fit with signal plus background functions.

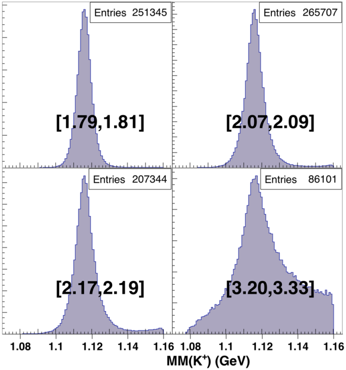

Event based dilution factor calculation for $\gamma p \rightarrow K^+ p(missing \pi^-)$

- Energy dependent MM(K^+)
- Q-factor method (A multivariant analysis)

  For each event ("seed event"), find N nearest neighbors in kinematic phase space (e.g. $\cos\theta^{cm}_{K^+}$, $\cos\theta^{cm}_{p}$, ϕ_p and W). Plot mass distribution of the $N+1$ events and fit with signal plus background functions.
- MM(K^+): W= 3.2- 3.33 GeV, weighted by Q for signal and by (1- Q) for background

total function (voigt + linear)
signal function (voigt)
background function (linear)

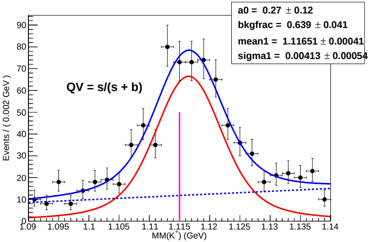

Figure : Seed event: Q-value fitting.

Event based dilution factor calculation for $\gamma p \rightarrow K^+ p(missing \pi^-)$

- Energy dependent MM(K^+)
- Q-factor method (A multivariant analysis)

  For each event ("seed event"), find N nearest neighbors in kinematic phase space (e.g. $\cos\theta^{cm}_{K^+}$, $\cos\theta^{cm}_{p}$, ϕ_p and W). Plot mass distribution of the $N+1$ events and fit with signal plus background functions.
- MM(K^+): W= 3.2- 3.33 GeV, weighted by Q for signal and by (1- Q) for background

MM(K^+)
MM(K^+)*Q
MM(K^+)*$(1-Q)$

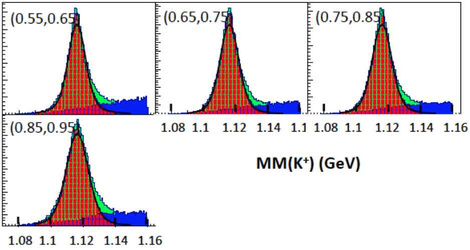

Measurement method: Maximum Likelihood

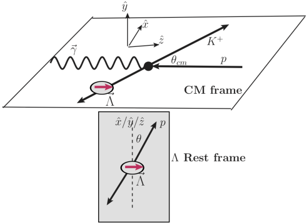

$$\hat{z} = \hat{p}_\gamma$$
$$\hat{y} = \frac{\hat{p}_\gamma \times \hat{p}_K}{|\hat{p}_\gamma \times \hat{p}_K|}$$
$$\hat{x} = \hat{y} \times \hat{z}$$

- Maximum Likelihood Method; – Event by event based method

$$\mathcal{L} = \prod_{i=1}^{N} [\mathcal{P}_i]^{w_i}$$

C_x, C_z: $w_i = Q_i$, $P_\odot$ photon beam polarization

$$\mathcal{P}(\cos\theta_x^p, \cos\theta_z^p | C_x, C_z)$$
$$= 1 \pm P_\odot \alpha (C_x \cos\theta_x^p + C_z \cos\theta_z^p)$$
$$-\log\mathcal{L} = -\sum_{i=1}^{N} Q_i \log(1 \pm P_\odot \alpha (C_x \cos\theta_x^p + C_z \cos\theta_z^p))$$

P: $w_i = Q_i \times f_{acc}^i$, α weak decay asymmetry = 0.642

$$\mathcal{P}(\cos\theta_y^p | P)$$
$$= 1 + \alpha P \cos\theta_y^p$$
$$-\log\mathcal{L} = -\sum_{i=1}^{N} Q_i f_{acc}^i \log(1 + \alpha P \cos\theta_y^p)$$

Outline

1. Introduction
   - Missing Baryon Problem
2. Experiment and Data Analysis
   - Experiment
   - Data Analysis
   - Measurement method
3. Results and Summary
   - Results comparison
   - Systematic uncertainty
   - Summary

Comparison: two-track and three-track topologies.

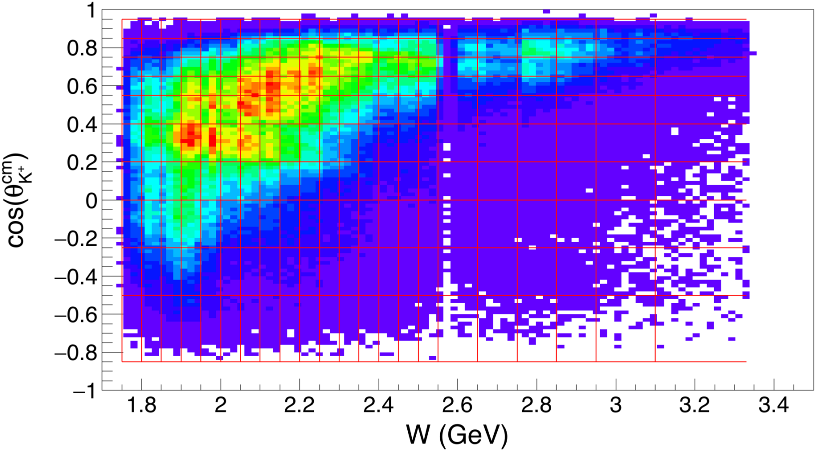

Figure : three-track; binning in W and $\cos\theta^{cm}_{K^+}$. $W = 23$, and $\cos\theta^{cm}_{K^+} = 10$

Comparison: two-track and three-track topologies.

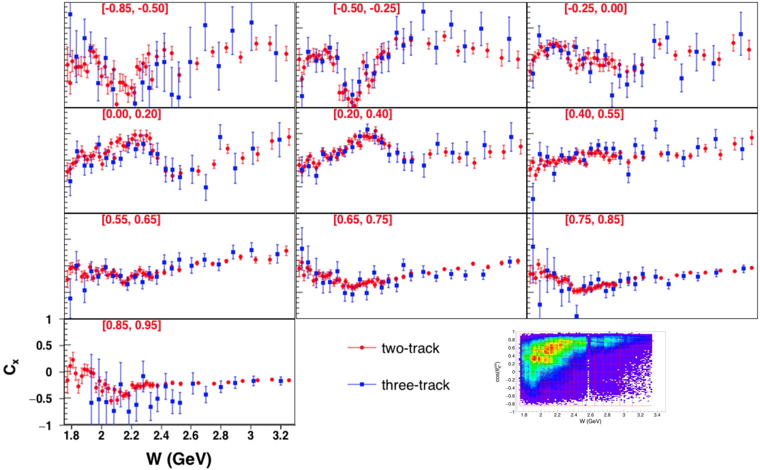

Comparison: two-track and three-track topologies.

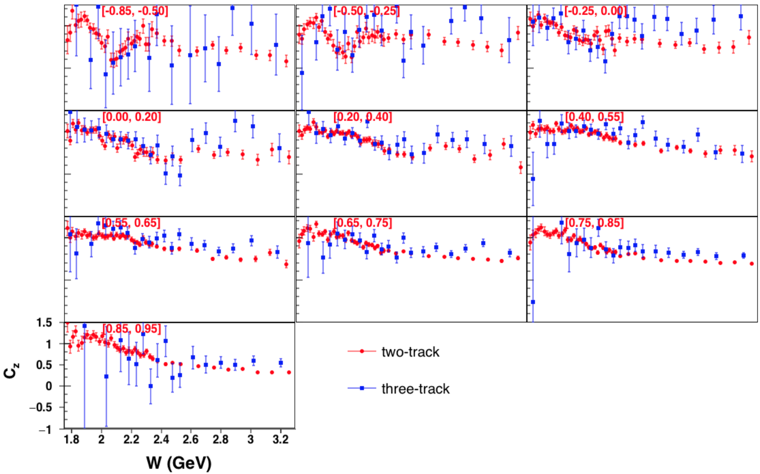

Comparison: two-track and three-track topologies.

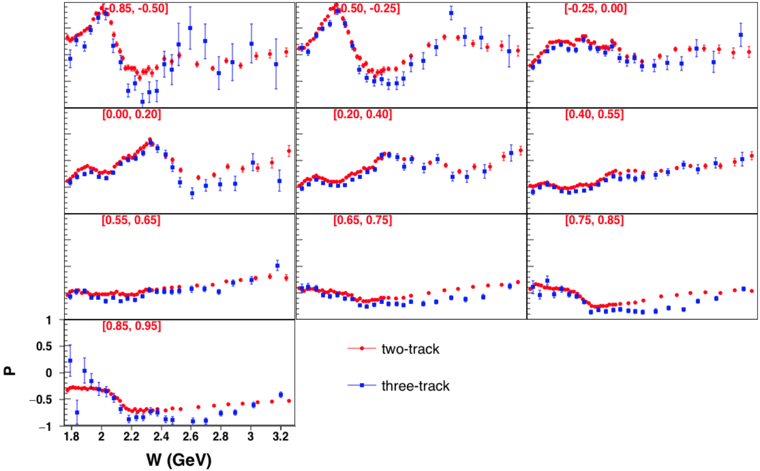

Comparison: two-track and three-track topologies.

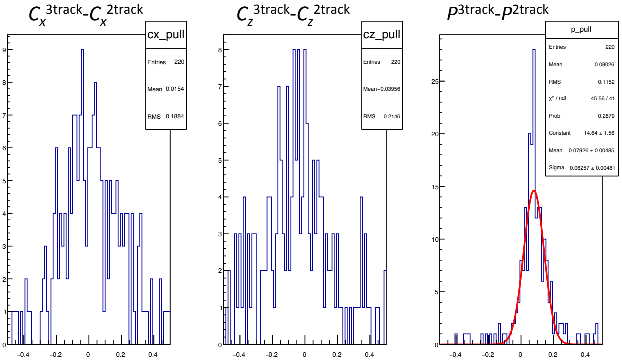

- Two-track preferred rather than three-track:
  – more statistics, better precision.
  – increased data point with smaller bin size.
  – background corrected using Q-factor method.
  – consistency check, suggested acceptance correction for P results.

Binning two-track

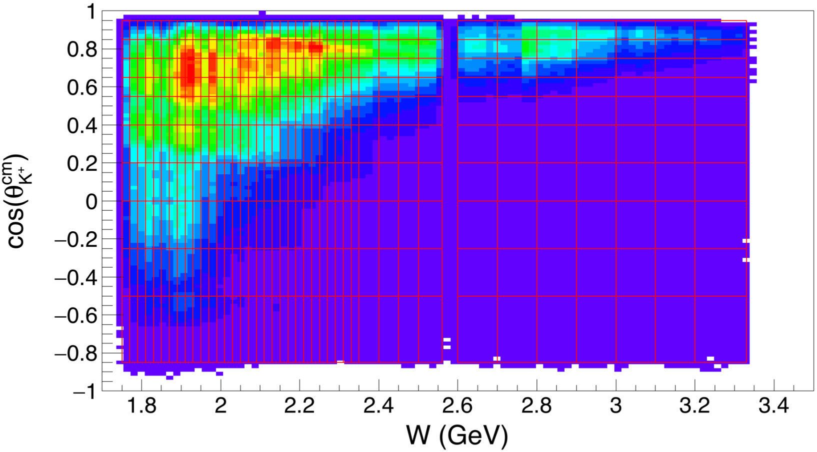

Figure : two-track, binning in W and $\cos\theta_{K^+}^{cm}$. $W = 41$, and $\cos\theta_{K^+}^{cm} = 10$

Comparing with Previous CLAS measurements

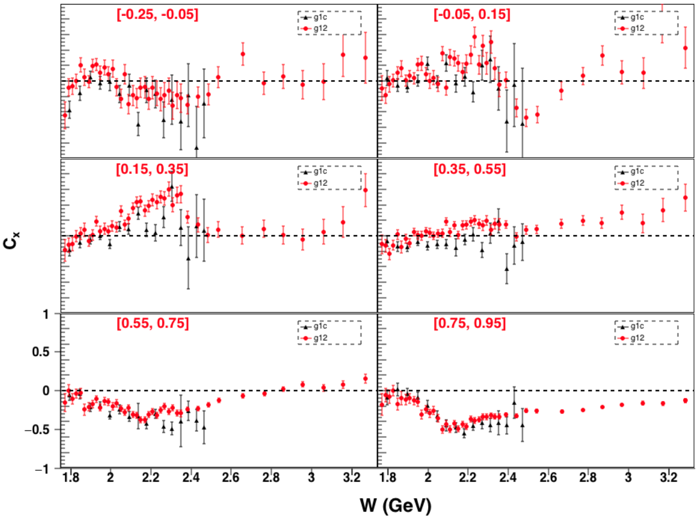

Comparing with Previous CLAS measurements

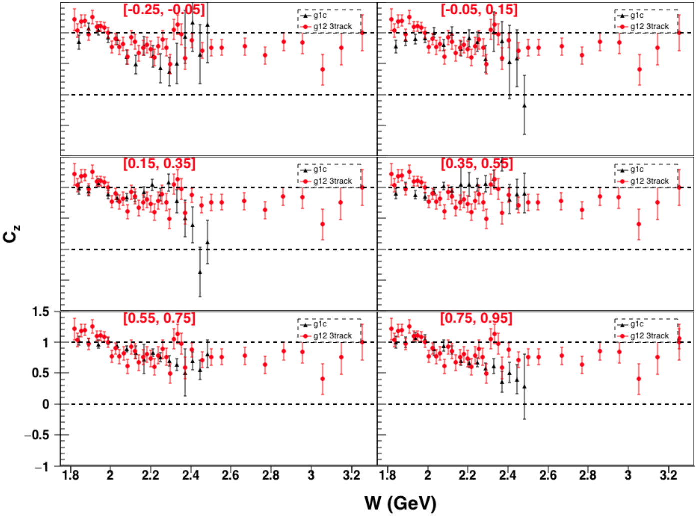

Comparing with Previous CLAS measurements

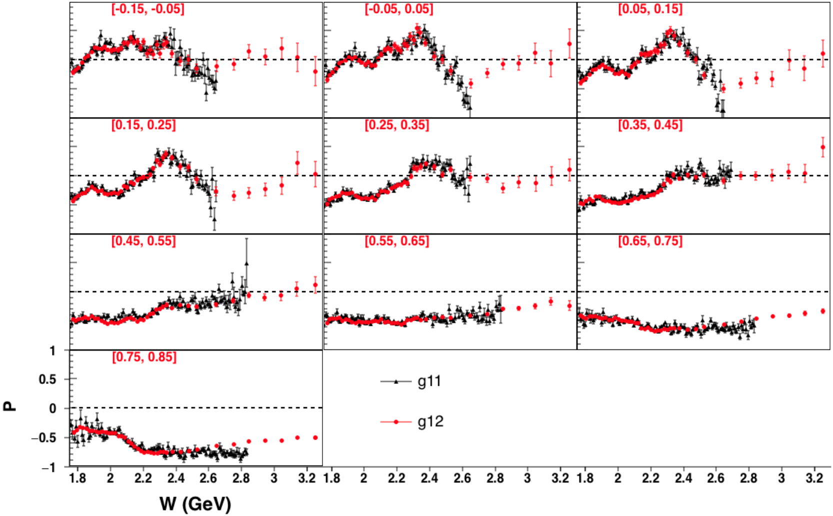

Comparing with Theory Model

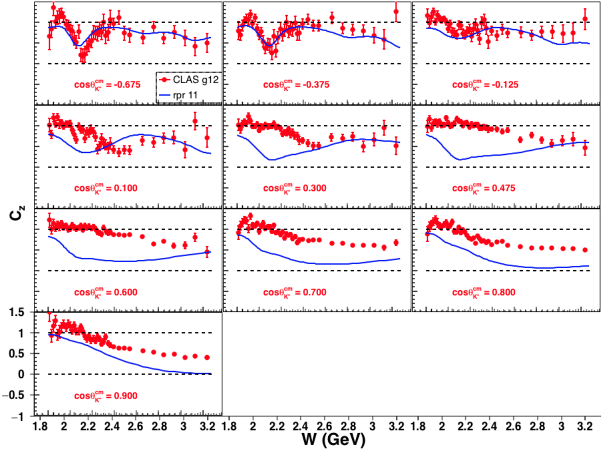

- Regge-Plus-Resonance Fit:
  – added t-channel contributions, exchange $K(494)$ and $K^*(892)$

RPR-2011 (PDG-2010)

- $S_{11}(1535)$ ★★★★
- $S_{11}(1650)$ ★★★★
- $D_{15}(1675)$ ★★★★
- $F_{15}(1680)$ ★★★★
- $D_{13}(1700)$ ★★★
- $P_{11}(1710)$ ★★★
- $P_{13}(1720)$ ★★★★
- $D_{13}(1875)$ m
- $P_{13}(1900)$ ★★
- $P_{11}(1900)$ m
- $F_{15}(2000)$ ★★★

Comparing with Theory Model

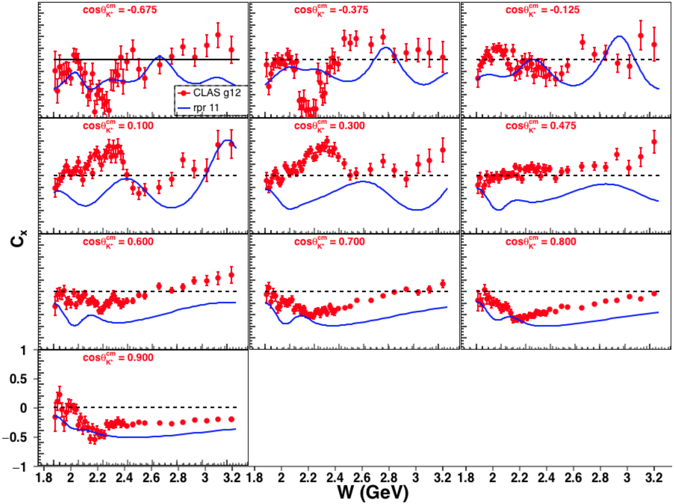

Systematic Uncertainty

Point-to-Point

- Cut related systematic uncertainty
  – Calculated variation selection criteria such as $\Delta t < 1$ ns to $\Delta t < 0.9$ ns.

$$\delta_{sys} = \sqrt{\frac{\sum_i \left(\frac{\mathcal{O}^i_{nom} - \mathcal{O}^i_{alt}}{\delta \mathcal{O}^i_{nom}}\right)^2}{\sum_i \left(\frac{1}{\delta \mathcal{O}^i_{nom}}\right)^2}},$$

- Uncertainty related to background
  – use Q-value $\pm\ \delta Q$.
- Total systematic uncertainty: $\delta_{sys,tot} = \sqrt{\sum_{src} \delta^2_{sys,src}}$

Scale Type

- Photon beam polarization
- Weak decay asymmetry α

Systematic Uncertainty

Point-to-point uncertainties			
Source	δP	δC_x	δC_z
timing cut	0.00126	0.00475	0.00420
vertex position cuts	0.0149	0.0126	0.00469
fiducial cuts	0.0085	0.0085	0.00417
confidence level cut	0.0109	0.0172	0.0236
Q-value	$3-7\%$	$3-5\%$	$3-7\%$
Scale-type uncertainties			
$P_\odot$	–	$0.05C_x$	$0.05C_z$
α	$0.020P$	$0.020C_x$	$0.020C_z$
Total	$0.020P$	$0.054C_x$	$0.054C_z$

Table : Systematic uncertainties for observables.

Summary

- Photoproduction of $K^+\Lambda$ is an important channel to investigate intermediate nuclear resonances.
- Polarization observables are important to disentangle overlapped states.
- Extended measurement for polarization observables– C_x, C_z, and P: – More data has been added to the previous measurements.
  – more precise measurement and great agreement with earlier CLAS results.
- Important to constrain the non-resonant (t-channel) contribution.
- Data are suitable to study the higher mass resonances.
- Further comparison with the different models, and collaboration with the theory group.

Thank You!

$\gamma p \to K^+\Lambda \to K^+ p\pi^-$

- Topologies for $K^+ p\pi^-$
  three-track: $\gamma p \to K^+ p\pi^-$ (no missing particle)
  two-track: $\gamma p \to K^+ p$ (missing π^-)
- Standard cuts and corrections

$\gamma p \to K^+\Lambda$; Λ, decay mode;
$p\pi^-$ 64%
$n\pi^\circ$ with 36%.
Final state K^+, proton, and π^- are required in data.

$\gamma p \to K^+\Lambda \to K^+ p\pi^-$

- Topologies for $K^+ p\pi^-$
  three-track: $\gamma p \to K^+ p\pi^-$ (no missing particle)
  two-track: $\gamma p \to K^+ p$ (missing π^-)
- Standard cuts and corrections
  - Timing cut

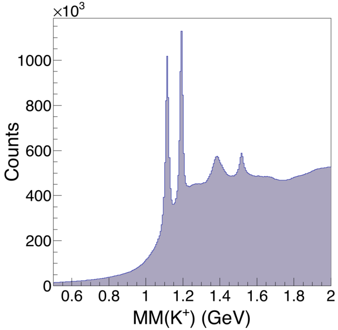

Missing mass of K^+ before cuts in $\gamma p \to K^+ p\pi^-$

$\gamma p \to K^+\Lambda \to K^+ p\pi^-$

- Topologies for $K^+ p\pi^-$
  three-track: $\gamma p \to K^+ p\pi^-$ (no missing particle)
  two-track: $\gamma p \to K^+ p$ (missing π^-)
- Standard cuts and corrections
  - Timing cut
  - Vertex cut

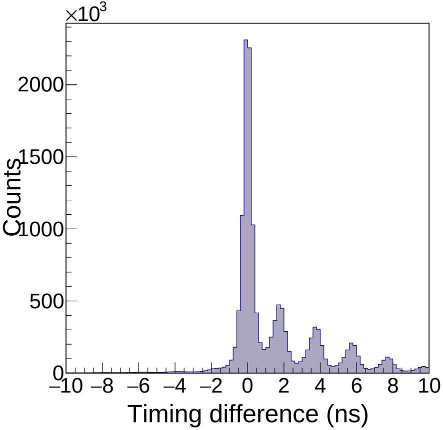

...to select right photon at vertex.
events are selected with ± 1 ns.

$\gamma p \to K^+\Lambda \to K^+ p\pi^-$

- Topologies for $K^+ p\pi^-$
  three-track: $\gamma p \to K^+ p\pi^-$ (no missing particle)
  two-track: $\gamma p \to K^+ p$ (missing π^-)
- Standard cuts and corrections
  - Timing cut
  - Vertex cut
  - Fiducial cut

Cut within the target length (40cm) + 5 cm downstream.

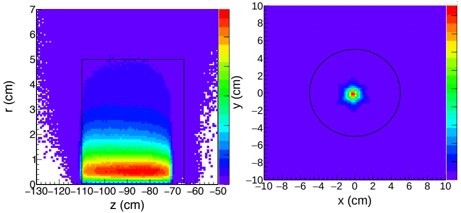

$\gamma p \to K^+\Lambda \to K^+ p\pi^-$

- Topologies for $K^+p\pi^-$
  three-track: $\gamma p \to K^+p\pi^-$ (no missing particle)
  two-track: $\gamma p \to K^+p$ (missing π^-)
- Standard cuts and corrections
  - Timing cut
  - Vertex cut
  - Fiducial cut
  - Time of Flight Knockout

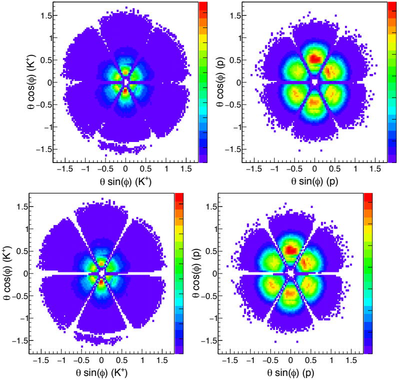

Loose, Nominal, and Tight; applied nominal cut.

$\gamma p \rightarrow K^+\Lambda \rightarrow K^+ p\pi^-$

- Topologies for $K^+ p\pi^-$
  three-track: $\gamma p \rightarrow K^+ p\pi^-$ (no missing particle)
  two-track: $\gamma p \rightarrow K^+ p$ (missing π^-)
- Standard cuts and corrections
  - Timing cut
  - Vertex cut
  - Fiducial cut
  - Time of Flight Knockout
  - Multiple Photon Cut

Table 3.2: List of removed paddles.

Sector 1:	6, 35, 40, 41, 50, 56
Sector 2:	2, 8, 34, 35, 41, 44, 50, 54, 56
Sector 3:	11, 35, 40, 41, 56
Sector 4:	41, 48
Sector 5:	48
Sector 6:	1, 5, 33, 56

Time of flight scintillator paddle number removed within six sector.

$\gamma p \to K^+\Lambda \to K^+ p\pi^-$

- Topologies for $K^+ p\pi^-$
  three-track: $\gamma p \to K^+ p\pi^-$ (no missing particle)
  two-track: $\gamma p \to K^+ p$ (missing π^-)
- Standard cuts and corrections
  - Timing cut
  - Vertex cut
  - Fiducial cut
  - Time of Flight Knockout
  - Multiple Photon Cut
  - E-p corrections

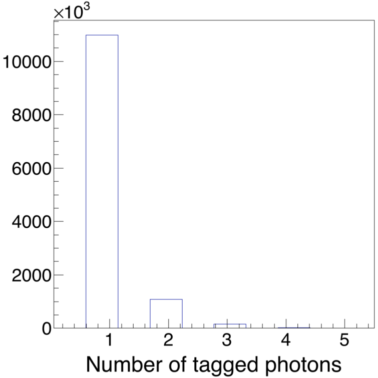

Only single photon events are selected.

$\gamma p \to K^+\Lambda \to K^+ p\pi^-$

- Topologies for $K^+ p\pi^-$
  three-track: $\gamma p \to K^+ p\pi^-$ (no missing particle)
  two-track: $\gamma p \to K^+ p$ (missing π^-)
- Standard cuts and corrections
  - Timing cut
  - Vertex cut
  - Fiducial cut
  - Time of Flight Knockout
  - Multiple Photon Cut
  - E-p corrections
- Kinematic fitting

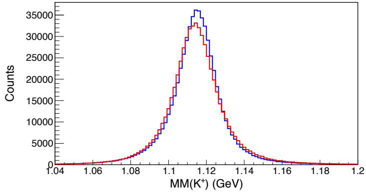

g12 momentum, photon beam energy, and energy loss of particle tracks are corrected. Collected effect. Red: before correction, Blue: after correction.

$\gamma p \to K^+\Lambda \to K^+ p\pi^-$

- Topologies for $K^+ p\pi^-$
  three-track: $\gamma p \to K^+ p\pi^-$ (no missing particle)
  two-track: $\gamma p \to K^+ p$ (missing π^-)
- Standard cuts and corrections
  - Timing cut
  - Vertex cut
  - Fiducial cut
  - Time of Flight Knockout
  - Multiple Photon Cut
  - E-p corrections
- Kinematic fitting
- Final Events

two-track: $CL > 5\%$

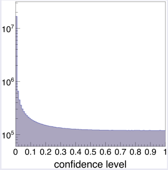

three-track: $CL > 1\%$

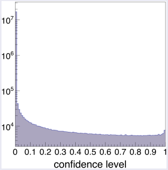

$\gamma p \to K^+\Lambda \to K^+ p\pi^-$

- Topologies for $K^+p\pi^-$
  three-track: $\gamma p \to K^+ p\pi^-$ (no missing particle)
  two-track: $\gamma p \to K^+ p$ (missing π^-)
- Standard cuts and corrections
  - Timing cut
  - Vertex cut
  - Fiducial cut
  - Time of Flight Knockout
  - Multiple Photon Cut
  - E-p corrections
- Kinematic fitting
- Final Events

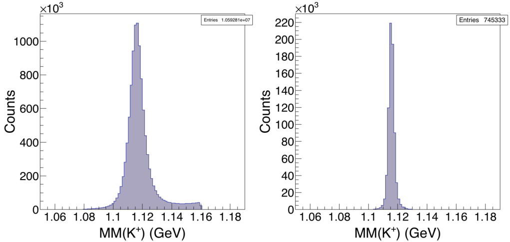

two-track : > 10 M
three-track : ≈ 0.75 M

$$R = \sqrt{(C_x^2 + C_z^2 + P^2)}.$$

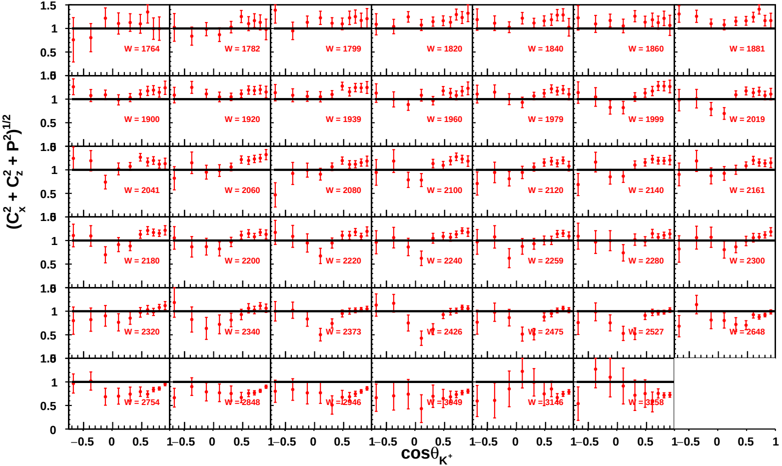

Final results with systematic uncertainty

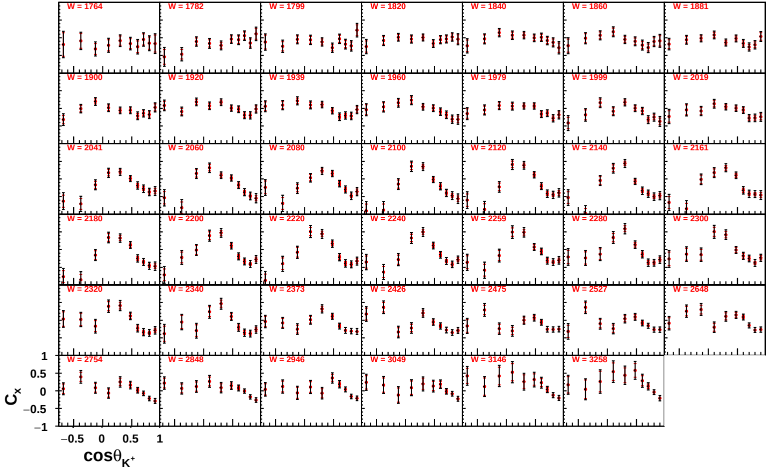

Final results with systematic uncertainty

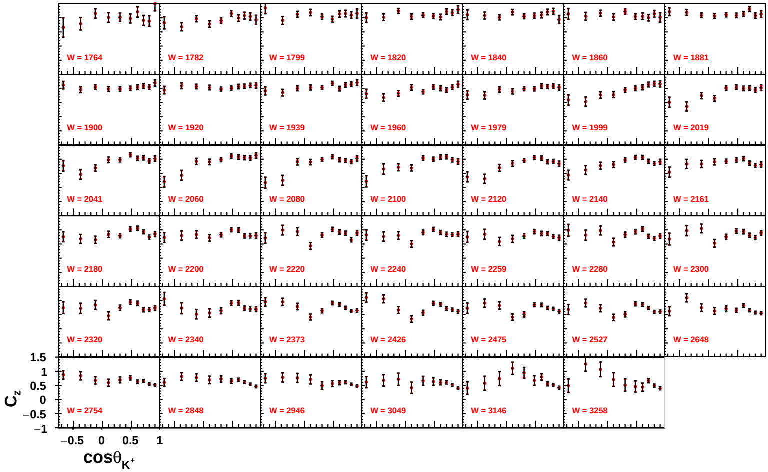

Final results with systematic uncertainty

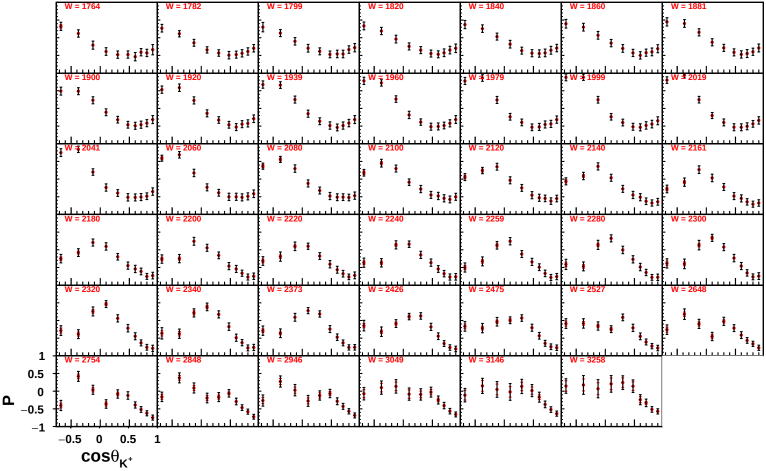

Effect of kinematic fitting

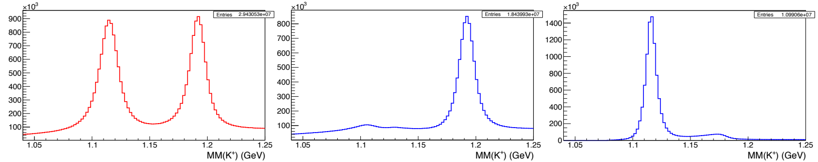

g12 running parameter

Table 3.1: Running conditions for *g12*

Electron Beam Energy	5.714 GeV
Electron Beam Current	60-65 nA (production) & 24 nA(single-prong)
Electron Beam Polarization	Circular
Radiator Material/Density	Au / 646 μg/cm^2
Radiator Thickness	$10^{-4}\chi_0$
Radius of Photon collimator	6.4 mm
Photon Beam Energy Range	1.142-5.425 GeV
Target Shell Material	Kapton
Target Length/Diameter	40 cm/4 cm
Target Material	ℓH_2
Target Position	-90 cm from CLAS center
Target Polarization	None
Torus Magnetic Current	$\frac{1}{2}B_{max} = 1930$ A